Properties of a wind farm wake as simulated by a numerical weather prediction model for the Smøla wind farm

by

Byrkjedal[1], Ø., Bredesen[1], R. E., Keck[2,3], R-E, Sondell[3], N. and Berge[1], E.
[1]Kjeller Vindteknikk AS, [2]University of Oslo, [3]Statkraft Development
oyvind.byrkjedal@vindteknikk.no tel: +47 48 09 95 30

Summary

Recently the numerical weather prediction model WRF (Weather Research and Forecasting) has been extended to account for wind farms in the mesoscale calculations by including the turbine drag coefficient. The wind farm will thus represent a sink of atmospheric momentum in the model. The scheme is implemented in the WRF model and as such the two way interaction between the wind farm and the atmosphere is described.

In the work presented here the kinetic energy converted into electrical energy from the Fitch scheme is compared to power production data from the 150 MW wind farm Smøla which consists of 68 turbines and is located in western Norway. The WRF model is run in the time domain for a period of 13 months from which we have concurrent data on power production from each turbine in the wind farm and data from a meteorological mast located near the wind farm. To simulations have been set up with the WRF model: Firstly, a reference simulation without a wind farm (REF) and secondly a simulation with the wind farm at Smøla simulated by the Fitch module (WAKE).

The influence of the wind farm as found from the mast observations is clearly seen also from the simulations. The positive wind speed bias found in the REF simulation is reduced in the WAKE simulation.

The data is classified by stability conditions. The wind speed deficits for both stable and unstable atmospheric conditions are shown. For stable conditions the wake extends further downstream compared to the unstable conditions. During unstable conditions the wake extends more vertically.

The energy that is converted to electrical energy in the WRF model is found to be underestimated by 7 % compared to the observations. The total wake loss calculated by the model is also underestimated.

1 Introduction

Recently the numerical weather prediction model WRF (Weather Research and Forecasting) has been extended to account for wind farms in the mesoscale calculations ([1], [2]) by including the turbine drag coefficient. The wind farm will thus represent a sink of atmospheric momentum in the model. The energy extracted from the available kinetic energy of the atmosphere is divided into two parts. Firstly kinetic energy is converted to electric energy which is expressed by the power coefficient. Secondly, kinetic energy is converted to turbulence which is expressed as an increase in the TKE (turbulent kinetic energy).

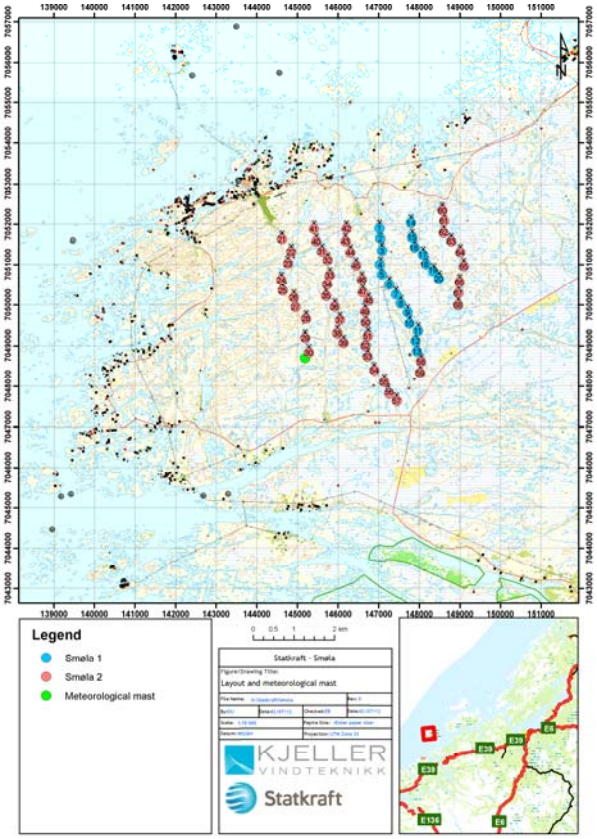

Figure 1 *Layout of Smøla wind farm*

The two way interaction between the wind farm and the atmosphere is described by the model and allows for studying how the wind farm influences on the local atmospheric conditions near the wind farm. This can be used to study how neighboring wind farms influence each other.

The wind farm Smøla is located on the Norwegian west coast. It consists of 68 turbines with an installed capacity of 150.4 MW. The layout of the wind farm is shown in Figure 1. A met mast is located near the south west corner of the wind farm. The distance from the mast to the nearest turbine is 2 rotor diameters, equivalent to 167 m. The wind farm was constructed during two phases, the combined wind farm Smøla 1 and Smøla 2 have been in operation since 2005.

2 Model description

2.1 Model setup

Two simulations have been carried out for the period June 2007 to July 2008 with the mesoscale model WRF (Weather Research and Forecasting). The model version used in this work is v3.5.0 described in [3]. One simulation is setup without influence of wind turbines and is referred to as the reference simulation, REF. The second simulation follows the exact same setup as REF, but with the wind farm at Smøla included. The latter simulation is referred to as the WAKE simulation.

The model is setup with 51 vertical layers, and 12 of the layers are located within the lowest 300 m of the atmosphere. The Mellor–Yamada–Nakanishi–Niino (MYNN2) 2.5 order turbulence scheme [4] is used to parameterize the boundary layer vertical mixing processes. The model employs 3 nested domains. The inner nest spans a grid with a total of 222 x 228 calculation points with a horizontal resolution of 1 km x 1 km. The location of the model domains is shown in Figure 2.

The model is run with data from ERA Interim reanalysis ([5]) as input on the boundaries.

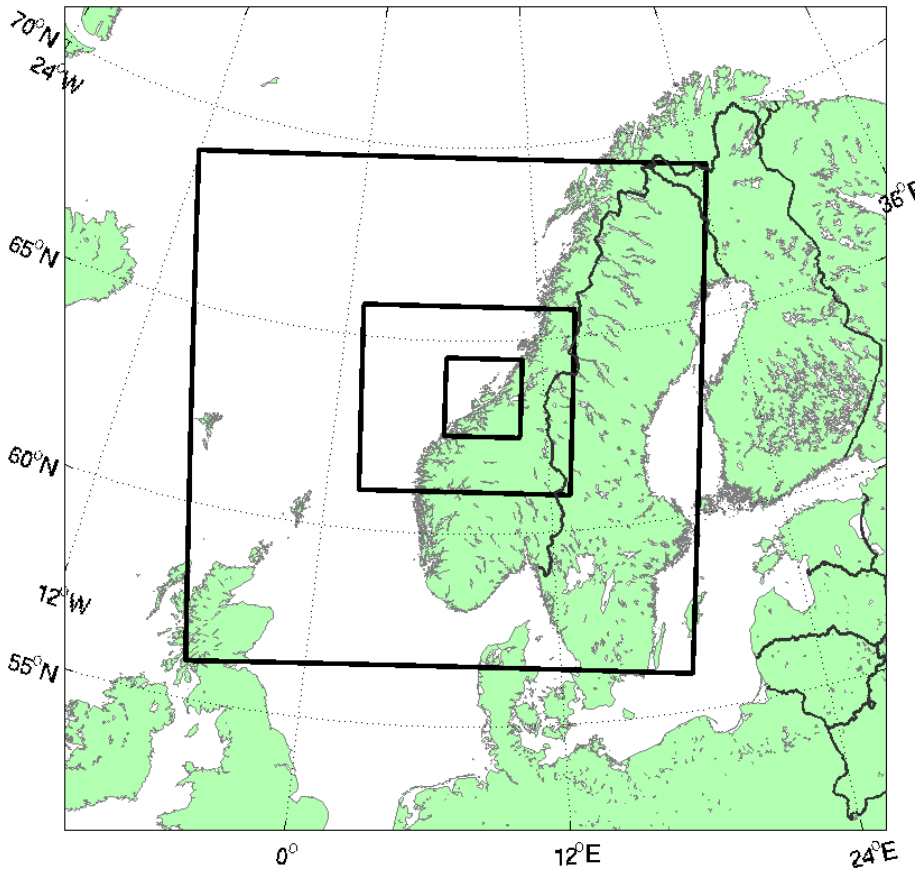

Figure 2 *Setup of the domains for the simulation*

2.2 Description of the Fitch module

For each grid point containing one or more wind turbines a calculation of the extracted energy is carried out. The change in kinetic energy is calculated for each of these grid points for each of the model level within the rotor plane of the turbines. This energy is proportional to the total rotor area within the grid point and model level. The intersection of the model levels on the rotor plane is illustrated in Figure 3. In our model setup the rotor plane is intersected by 5 model levels.

The change of kinetic energy from the Fitch module is described as follows (the description is taken from [1]): The rate of change of Kinetic Energy within grid cell i,j,k is equal to the rate of loss of Kinetic energy due to wind turbines in that cell:

$$\frac{\partial |\mathbf{V}|_{ijk}}{\partial t} = -\frac{\frac{1}{2} N_t^{ij} C_T(|\mathbf{V}|_{ijk}) |\mathbf{V}|_{ijk}^2 A_{ijk}}{(z_{k+1} - z_k)} \quad (1)$$

Here $|\mathbf{V}|_{ijk}$ is the scalar wind speed within model grid i,j,k. C_T is a the thrust coefficient dependent on wind speed. N_t^{ij} is the sum of installed power within grid i,j. N_t is equal to the number of turbines multiplied by rated power. A_{ijk} is the swept area of one turbine within model grid i,j,k. $(z_{k+1} - z_k)$ refers to the thickness of the model layer.

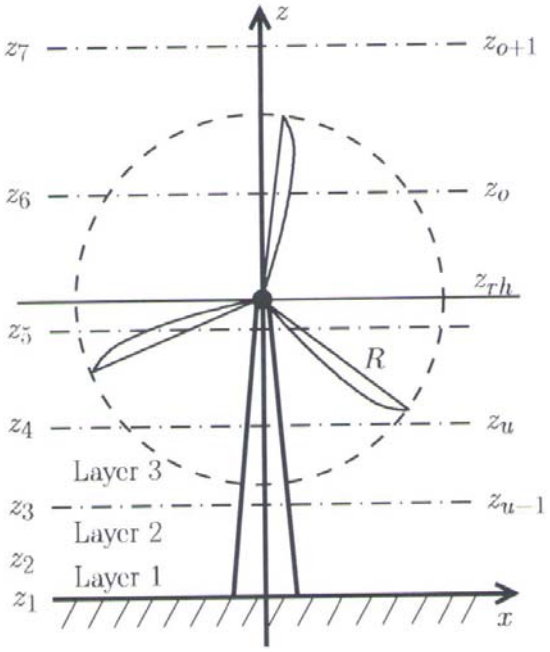

Figure 3 *Schematic description of a wind turbine and a typical vertical configuration of a meso scale model. The indexing of the layers is from bottom to top. z_{rh} is the rotor hub height. R is the rotor radius. The Figure is taken from [6].*

The energy per unit mass which is extracted by the turbines and is converted to electrical energy, and is given by:

$$\frac{\partial P_{ijk}}{\partial t} = -\frac{\frac{1}{2}N_t^{ij}C_P(|\mathbf{V}|_{ijk})|\mathbf{V}|_{ijk}^3 A_{ijk}}{(z_{k+1}-z_k)} \quad (2)$$

The energy per unit mass which is extracted from the atmosphere by the wind farm and converted to turbulent kinetic energy TKE is expressed by:

$$\frac{\partial TKE_{ijk}}{\partial t} = -\frac{\frac{1}{2}N_t^{ij}C_{TKE}(|\mathbf{V}|_{ijk})|\mathbf{V}|_{ijk}^3 A_{ijk}}{(z_{k+1}-z_k)} \quad (3)$$

The power coefficient, C_P, which represents the energy of the air flow which is converted to useful electrical energy can be expressed by:

$$C_P = C_T - C_{TKE} \quad (4)$$

3 Results

3.1 Mast observations

The wind rose from the mast observations are shown in Figure 4 (left panel). The main wind direction is from the south west. One can clearly see the influence of the wind farm on the observations. In particular for winds from the northeast we find the largest frequency of low wind speeds (< 10 m/s). The wind rose from the WRF model (WAKE) is shown in the right panel of Figure 4. The model generally describes the wind direction distribution quite well and also the distribution of wind speed in each sector except for sector 2 (30 degrees) where the wind farm influence on the met mast is expected to be the largest, and a very strong influence of the turbine closest to the met. mast is found.

It must also be noted that the distance from the mast to the first turbine (turbine 30) is only 2 rotor diameters (approximately 167 m). The grid point that has been chosen to represent the met mast from the WRF model data is located southwest of the wind farm at a distance of 1400 m from the first grid point containing a wind turbine.

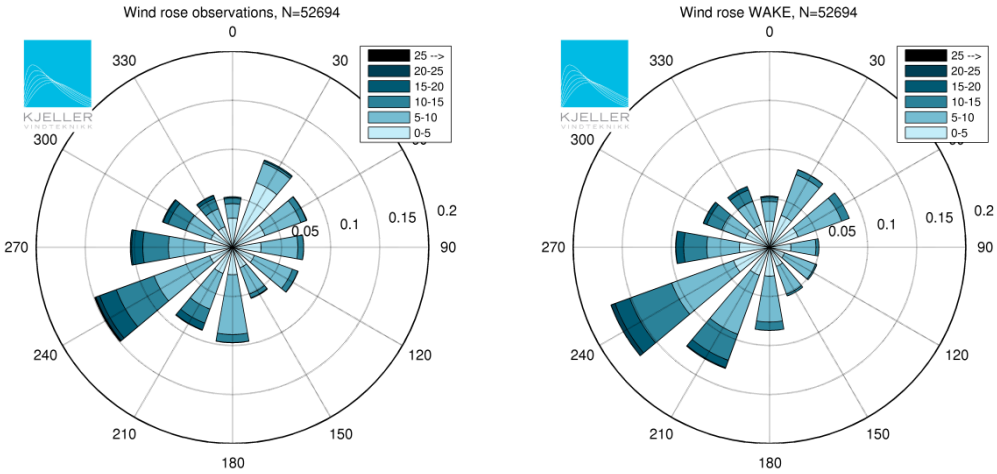

Figure 4 *Wind rose from the observations (left) and from the model (right)*

The average wind speed for different wind direction is shown in Figure 5. The figure shows the observed wind speed given in red color, while the wind speed from the REF and WAKE model runs for this location is shown as black curves. The model data clearly shows the wind speed deficit caused by the wind farm for 0-120 degrees. The magnitude of the wind speed deficit is up to 1.5 m/s at this location. For comparison the observations show that the average wind speed is very low for winds in the direction 0-50 degrees.

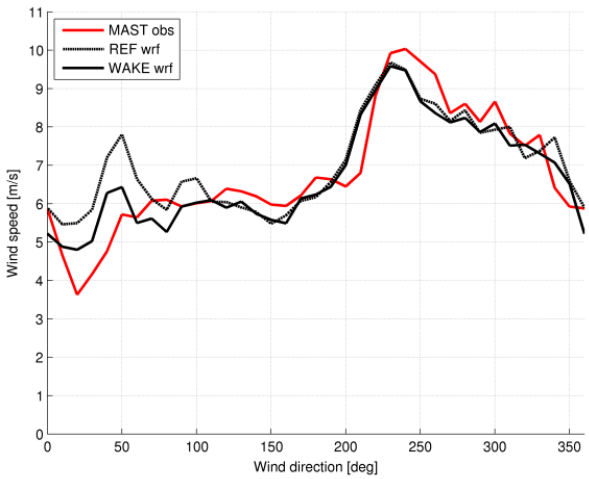

Figure 5 *Average wind speed for different wind directions. The red curve shows the observed wind speed. The black curve shows the wind speed for the WAKE simulation, while the dotted curve is for the REF simulation*

Table 1 shows a comparison of the measured wind speed with the WAKE and REF simulations. The REF simulation shows a positive bias of 5 % compared to the observations. For the WAKE simulation the bias is reduced to 1 %. It is also shown that the MAE is lower for the WAKE simulation compared to REF, while the correlation is somewhat higher.

Figure 6 shows the pressure perturbation that is caused by the wind farm in the simulations. The wind farm itself represents a positive pressure perturbation. The increased pressure over the wind farm will cause a deflection of the winds around (or over and under) the wind farm. A negative perturbation can be seen in the wake of the wind farm. The positive perturbation of the wind farms extends also some distance upstream of the wind farm. By comparing the mast observations with the nacelle anemometers evidence of a blockage effect has been found for some wind directions. The pressure perturbation field suggests a blockage effect of the wind farm as a whole causing the air to deflect around the wind farm.

Table 1 *Bias, mean absolute error and correlation coefficient between simulations and observations.*

	REF	WAKE
bias	4.8 %	0.8 %
mean absolute error (MAE)	27.8 %	26.1 %
correlation coefficient (r)	0.79	0.80

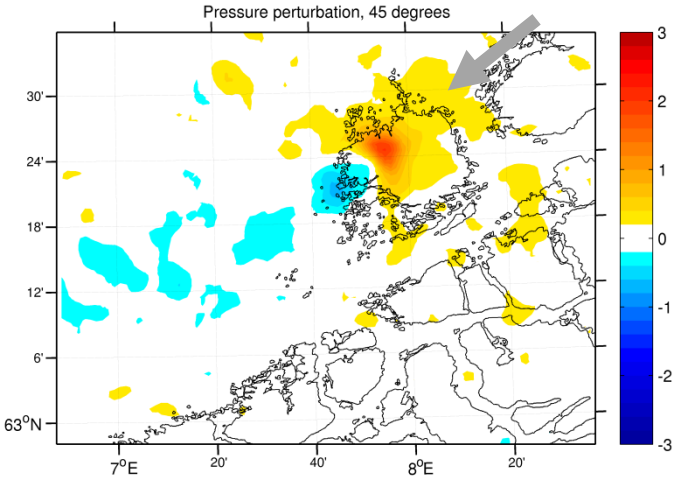

Figure 6 *Pressure perturbation [Pa] caused by the wind farm for winds from north east*

3.2 Stability conditions

Atmospheric stability will influence on the magnitude of the wake losses in the wind farm. Such dependency is shown for Horns Rev in e.g. [7]. For Smøla we calculate the atmospheric stability from the vertical temperature profile from the WRF simulations. We define the unstable cases as cases where the potential temperature gradient is lower than -0.2 K/100m. The stable conditions are defined as the cases with potential temperature gradient above 0.2 K/100m. The temperature gradient is calculated across model levels from approximately 12m to 138m. The neutral cases are the ones with potential temperature gradient between the two limits described here. The definition used and the frequency of each stability class are shown in Table 2. The classification shows that stable conditions are the most prevailing at this site accounting for 68.2 % of the time. Unstable conditions are found only for 7.0 % of the time. These are values from the model. There are no observations of the vertical temperature gradient at the site.

Table 2 *Definition of stability classes used in the analysis and frequency of occurrence for each class. θ denote the potential temperature.*

	Definition	Frequency
Stable	$d\theta > 0.2$ K/100m	68.2 %
Neutral	$-0.2 < d\theta < 0.2$ K/100m	24.8 %
Unstable	$d\theta < -0.2$ K/100m	7.0 %

The modeled wind roses for unstable, neutral and stable conditions are shown in Figure 7. The highest frequency of unstable conditions is related to winds from the northeast. Neutral conditions are most common with southwest and also from all cases with winds from the ocean (west to northeast). Stable conditions are most common for southwest wind directions, but often also related to winds from land (south to east).

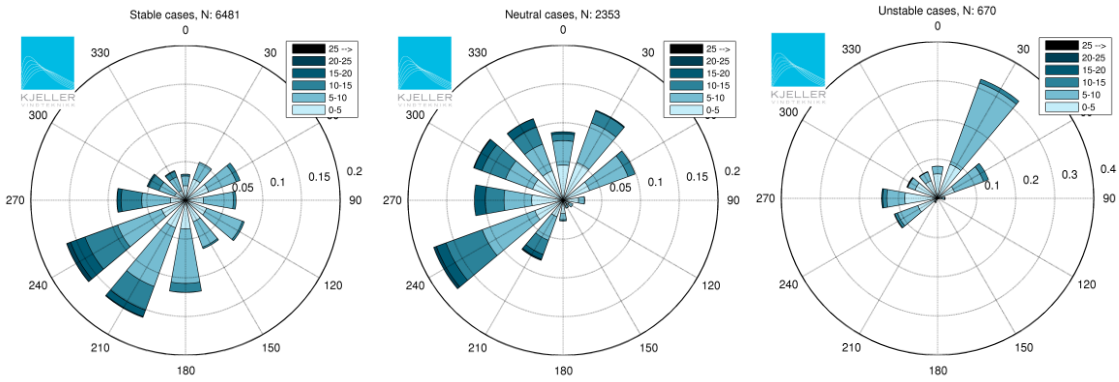

Figure 7 Wind roses for the stable (left), neutral (mid) and unstable (right) conditions from the WAKE simulation. The number of cases in each class (N) is also given.

The highest frequency of unstable conditions is found with winds from the northeast. To analyze the difference in wake properties in stable and unstable conditions we chose to study the cases with winds with in the sector defined as 45°± 22.5°. We use only the cases with wind speeds in the range 5-15 m/s to avoid the different wind speed distributions that can be found during stable and unstable conditions. The modeled average wind speed deficit for stable and unstable conditions for this sector is shown in Figure 8 and Figure 9. We find 208 cases with unstable conditions and 385 cases with stable conditions, the average wind speed for the two classes are 7.3 m/s and 7.0 m/s respectively. The wind speed deficit is clearly larger and reaches longer distances under stable conditions compared to the unstable conditions. For stable conditions we find a wind speed deficit of 0.3 m/s 20-25 km downstream of the wind farm for this defined sector. For the unstable conditions the wind speed deficit is smaller than 0.3 m/s 10-15 km downstream of the wind farm.

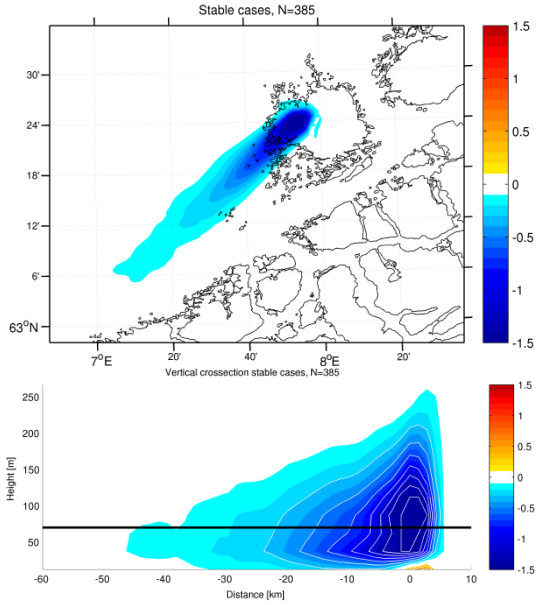

Figure 8 *Wind speed deficit for stable conditions with winds from sector 45°± 22.5°. The upper figure shows deficit at hub height (70 m). The lower figure shows the vertical cross section. The SW corner of the wind farm is at 0 km. The units are in m/s.*

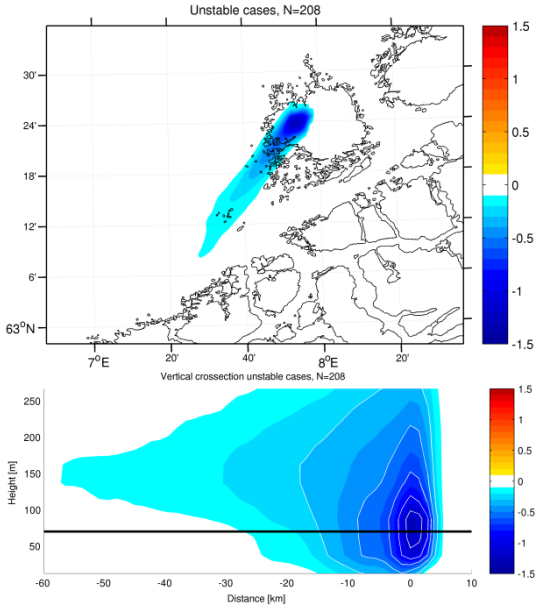

Figure 9 Wind speed deficit for unstable conditions with winds from sector 45°± 22.5°. The upper figure shows deficit at hub height (70 m). The lower figure shows the vertical cross section. The SW corner of the wind farm is at 0 km. The units are in m/s.

The vertical cross sections of the wind speed deficit along the 45° sector for the stable and unstable conditions are shown in the lower panels of Figure 8 and Figure 9. It is clearly shown that the wake propagates more vertically during the unstable conditions compared to the stable conditions. One can also note an increase in wind speed for the lowest model level in the stable cases. This represents an increase of the wind speed below the rotor plane of the turbines. However, as the wake is dispersed vertically this feature is quickly reduced in the wind farm.

3.3 Power Calculations

Using the equations (1-4) which describes the energy that has been extracted from air flow using the Fitch module, the power produced by the wind farm can be estimated. By comparing the WAKE simulation by the REF simulation we also estimate the total wake loss in the wind farm. The "observed" wake loss is also calculated from the wind farm SCADA data, by using the anemometer data from the met mast and transfer functions between the met mast and each single turbine ([8]).

The calculations with the WRF model generally underestimate the power produced from the wind farm. As a total for the 13 month simulation period the underestimation in power from the WRF calculation is 7.3 %. The wake losses are also underestimated by the WRF model as shown in Table 3.

Table 3 Comparison of modeled and observed power and wake loss for the period July 2007 until July 2008.

	Model	Observed
Power	-7.3 %	
Wake loss	10.5 %	13.1 %

The underestimation of the power may be related to the simplified power curve that is implemented in the Fitch module. The implemented C_P curve gives a lower conversion of energy to electrical energy compared to the C_P curve of the turbines installed in the wind farm. The lower power output estimated from the wind farm can also be caused by underestimation of wind velocities.

The wake losses are too small compared to the actual wake losses in the wind farm. This can be related to the simplified C_T curve that is used by the model, but also the fact that the model contains several turbines within each grid point. The model does not include any sub-grid parameterization of the turbines, meaning that the turbines will not influence the power production for other turbines within the same grid point.

4 Conclusions

The Fitch module ([1]) is found to be a useful tool to study the mesoscale effects of a wind farm. The scheme is implemented in the WRF model and as such the two way interaction between the wind farm and the atmosphere is described.

The 150 MW wind farm Smøla has been simulated. The wind speed deficits for both stable and unstable atmospheric conditions are shown. For stable conditions the wake extends further downstream compared to the unstable conditions. During unstable conditions the wake extends more vertically.

The energy that is converted to electrical energy in the WRF model is found to be underestimated compared to the observations. The total wake loss calculated by the model is also underestimated.

5 Acknowledgements

The simulations were performed on the Abel Cluster, owned by the University of Oslo and the Norwegian meta center for High Performance Computing (NOTUR), and operated by the Department for Research Computing at USIT, the University of Oslo IT-department. http://www.hpc.uio.no/. The work has been founded by the Norwegian Research Council.

6 References

1. Fitch, A.C., J.B. Olson, J.K. Lundquist, J. Dudhia, A.K. Gupta, J. Michalakes, and I. Barstad, 2012: Local and mesoscale impacts of wind farms as parameterized in a mesoscale NWP model. Monthly Weather Review, 140, 3017-3038

2. Fitch, A.C., J.B. Olson, J.K. Lundquist, J. Dudhia, A.K. Gupta, J. Michalakes, and I. Barstad, 2013: Corrigendum. Monthly Weather Review, 141, 1395–1395

3. Skamarock WC, Klemp JB, Dudhia J, Gill DO, Barker DM, Duda MG, Huang X-Y, Wang W. and Powers JG, 2008: A Description of the Advanced Research WRF Version 3, NCAR Technical Note NCAR/TN-475+STR, Boulder, June 2008

4. Nakanishi, M., and H. Niino, 2009: Development of an improved turbulence closure model for the atmospheric boundary layer. J. Meteor. Soc. Japan, 87, 895–912

5. Dee, D. P., et al. (2011), The ERA-Interim reanalysis: configuration and performance of the data assimilation system. Q.J.R. Meteorol. Soc., 137: 553–597. doi: 10.1002/qj.828

6. Blahak, U., B. Goretzki, and J. Meis, 2010: A simple parameterization of drag forces induced by large wind farms for numerical weather predictionmodels. Proc. EuropeanWindEnergy Conf. and Exhibition 2010, PO ID 445, Warsaw, Poland, EWEC, 186–189.

7. Hansen, K.S., R.J. Barthelmie, L.E. Jensen and A. Sommer, 2012: The impact of turbulence intensity and atmospheric stability on power deficits due to wind turbine wakes at Horns Rev wind farm, Wind Energy, 15, 183–196

8. Undheim O., R-E Keck, E. Berge, L. Rognlien and M. Håkansson 2014: Time-dependent wind energy calculations. Poster no 306, EWEA 2014